Dental Depth Profilometric Diagnosis of Pit & Fissure Caries using Frequency-Domain Infrared Photothermal Radiometry and Modulated Laser Luminescence

Raymond J. Jeon[a], Andreas Mandelis[*a], Victor Sanchez[a] and Stephen H. Abrams[b]
[a]Center for Advanced Diffusion-Wave Technologies (CADIFT), Dept. of Mechanical and Industrial Engineering, Univ. of Toronto, 5 King's College Road, Toronto, Ontario, M5S 3G8, Canada;
[b]Four Cell Consulting, 748 Briar Hill Ave., Toronto, Ontario, M6B 1L3, Canada

ABSTRACT

Non-intrusive, non-contacting frequency-domain photothermal radiometry (FD-PTR or PTR) and frequency-domain luminescence (FD-LUM or LUM) have been used with 659- nm and 830-nm laser sources to detect artificial and natural sub-surface defects in human teeth. Fifty-two human teeth were examined with simultaneous measurements of PTR and LUM with the 659-nm laser and compared to conventional diagnostic methods including continuous (dc) luminescence (DIAGNOdent), visual inspection and radiographs. To compare each method, sensitivities and specificities were calculated by using histological observations as the gold standard. With the combined criteria of four PTR and LUM signals (two amplitudes and two phases), it was found that the sensitivity of this method was much higher than any of the other methods used in this study, whereas the specificity was comparable to that of dc luminescence diagnostics. Therefore, PTR and LUM, as a combined technique, has the potential to be a reliable tool to diagnose early pit and fissure caries and could provide detailed information about deep lesions with its depth profilometric character. Also, from the experiments with the teeth having natural or artificial defect, some depth profilometric characteristics were confirmed. The major findings are (i) PTR is sensitive to very deep (>5 mm) defects at low modulation frequencies (5 Hz). Both PTR and LUM amplitudes exhibit a peak at tooth thicknesses ca. 1.4 - 2.7 mm. Furthermore the LUM amplitude exhibits a small trough at ca. 2.5~3.5 mm; (ii) PTR is sensitive to various defects such as a deep carious lesion, a demineralized area, and a crack while LUM exhibits low sensitivity and spatial resolution.

Keywords: dental photothermal radiometry, modulated luminescence, dental caries diagnosis, pit and fissure caries, depth profilometry, frequency scans

1. INTRODUCTION

Over the last few decades with the widespread use of fluoride, the prevalence of caries, particularly smooth surface caries has been considerably reduced[1]. This reduction in smooth surface caries has resulted in an increase in the proportion of small lesions in the pits and fissures of teeth[1]. The diagnosis of pit and fissure caries continues to be a dilemma for clinicians. The development of a non-invasive, non-contacting technique or instrument which can detect early demineralization on or beneath the enamel surface is essential for the clinical management of this problem.

The use of lasers for dental diagnostics is considered to be promising, mainly through the phenomenon of laser-induced fluorescence of the enamel or the fluorescence caused by porphyrins present in carious tissue[2-6].

The first attempt to apply the depth profilometric capability of frequency-domain laser infrared photothermal radiometry (PTR) toward the inspection of dental defects was reported by Mandelis et al.[7] and Nicolaides et al.[8] and was recently reviewed by Mandelis[9]. The approach of these investigators consists of a combined dynamic (i.e. non-static, steady-state signal level) dental depth profilometric inspection technique, which can provide simultaneous measurements of intensity-modulated frequency-domain PTR (FD-PTR) and luminescence (FD-LUM) signals from defects in teeth. FD-PTR is an evolving technology and has been applied, among other areas, to the non-destructive evaluation (NDE) of sub-surface features in opaque materials[10]. The technique is based on the modulated thermal infrared (black-body or Planck radiation) response of a medium, resulting from radiation absorption and non-radiative

* mandelis@mie.utoronto.ca; phone 1 416 978-5106; fax 1 416 978-7753

Photons Plus Ultrasound: Imaging and Sensing, edited by
Alexander A. Oraevsky, Lihong V. Wang, Proceedings of SPIE Vol. 5320
(SPIE, Bellingham, WA, 2004) 1605-7422/04/$15 · doi: 10.1117/12.537854

energy conversion followed by a small temperature rise. The generated signals carry sub-surface information in the form of a temperature depth integral. Thus, PTR has the ability to penetrate, and yield information about, an opaque medium well beyond the range of optical imaging. Specifically, the frequency dependence of the penetration depth of thermal waves makes it possible to perform depth profiling of materials[11]. In PTR appications to turbid media, such as hard dental tissue, depth information is obtained following optical-to-thermal energy conversion and transport of the incident laser power in two distinct modes: conductively, from a near-surface distance (50 ~ 500 μm) controlled by the thermal diffusivity of enamel; and radiatively, through blackbody emissions from considerably deeper regions commensurate with the optical penetration of the diffusely scattered laser-induced optical field (several mm)[12].

It is often desirable in dental practice to obtain detailed information on potential lesions or to examine pits and fissures with high spatial resolution, using a focused laser source. To meet these objectives, recently, a combination of FD-PTR and FD-LUM was used as a fast dental diagnostic tool to quantify sound enamel or dentin as well as sub-surface cracks in human teeth[8]. More recently, it was found that PTR (alone or in combination with LUM) could be used as a sensitive, depth-profilometric dental probe for the diagnosis of near-surface or deep sub-surface carious lesions and/or for monitoring enamel thickness[13].

In this study, fifty two human teeth were examined to evaluate the diagnostic capabilities of FD-PTR and FD-LUM and compared to DIAGNOdent as well as visual inspection and radiographs. After the measurements were completed, the teeth were sectioned and histological findings were used as the gold standard to calculate and compare the sensitivity and the specificity of all the diagnostic methodologies used in this study. Also, various natural defects has been examined with this technology, and in order to investigate whether an artificially drilled hole can influence either the PTR or the LUM signals, spatial scans on a side surface of a tooth were performed with the 659-nm laser at 5 Hz after gradual drilling of a hole from the opposite side.

2. EXPERIMENTAL METHOD

Fifty two extracted human teeth were evaluated. The measured points included, at a minimum, two healthy areas and two fissures on the occlusal surface and one healthy point on the smooth side surface. A few more measured points were added for each tooth, so the total measurement sample finally consisted of 332 points, including 104 healthy points, 176 fissures on the occlusal surface, and 52 healthy points on the smooth surfaces of the teeth. In order to compare our experimental results to other clinical methods, 5 dentists examined and ranked the set of teeth by visual inspection and radiographs. DIAGNOdent (KAVO Model 2095) measurements were also obtained from the occlusal surfaces of the teeth.

2.1 Visual Inspection and Radiographic Examination

The clinicians were asked to assign a ranking from 1 to 10 for each tooth with 1 meaning no treatment was required and 10 meaning that a large carious lesion was present involving the dentin and enamel (see Table 1). The clinicians were not asked to assess each fissure, only to rank the status of all fissures on the occlusal surface. Rankings were further divided into four groups with the classification scheme described in Table 1.

A radiograph was taken on each tooth using standard dental x-rays. Each radiograph was examined by the clinicians to detect the presence of occlusal caries.

2.2 DIAGNOdent

Each tooth was dried and the DIAGNOdent instrument was used to obtain readings from the occlusal surface. The machine was calibrated between each tooth and the surface was scanned three times to confirm the reading. The highest reading and its location were recorded. The readings were assessed and ranked using the criteria developed by Lussi et al.[6] and listed in Table 1.

2.3 Sample Preparation before PTR and LUM Scanning

Each sample tooth in the study was removed from the vial and was rinsed thoroughly with clean water for more than 20 seconds and then was dried with pressurized air. Then, the tooth was placed on the sample stage, and the laser was turned on and focused on the sample tooth by adjusting a 3-axis micrometer stage. This process usually took about

20 minutes before starting measurements, during which time the tooth was dehydrated properly. Moreover, since the surface temperature of the sample could be slightly decreased during washing with water and drying with compressed air, there was a need to wait until the sample temperature reached its ambient value, because modulated luminescence and thermal infrared (blackbody) emissions may be affected by the background temperature.

Table 1. Diagnostic criteria for the Visual Inspection, DIAGNOdent, X-ray and Histological Observation

General Description of Levels of Caries	Visual Inspection (1~10)	DIAGNOdent (0~99) [6]	Radiograph	Histological Observation
D_0: Intact			Healthy: Indicating no sign of demineralization	Sound enamel or Healthy fissure
D_1: no caries, or histological enamel caries limited to the outer half of the enamel thickness	1 ~ 2 Incipient or Healthy Fissures Observe & Monitor	0-4	Enamel caries under 1/2 the distance to DEJ	Demineralized fissure but solid enamel base; very good enamel thickness to the pulp; at least 1/2 thickness of enamel remains intact
D_2: histological caries extending beyond the outer half, but confined to the enamel	3 ~ 5 Fissures are suspect. Fissure Sealant recommended	4.01 ~ 10	Enamel caries greater than 1/2 the distance to DEJ	Demineralized fissure but solid enamel base
D_3: histological dentinal caries limited to the outer half of the dentin thickness	6 ~ 8 Restore the Fissure with direct placed restoration	10.01 ~ 18	Dentin caries	Caries into dentin
D_4: histological dentinal caries extending into the inner half of dentin thickness	9 ~ 10 Deep Dentin Caries Large carious lesions	> 18.01		

2.4 PTR and LUM Measurements

Fig. 1 shows the experimental setup for combined frequency-domain PTR and LUM probing. Two semiconductor lasers with wavelength 659 nm (maximum power 30 mW; Mitsubishi ML1016R-01) and with 830-nm (maximum power 100 mW, Sanyo DL-7032-001) were used as the sources of both PTR and LUM signals. A diode laser driver (Coherent 6060) was used for both lasers and was triggered by the built-in function generator of the lock-in amplifier (Stanford Research SR830), modulating the laser current harmonically. The laser beam was focused on the sample with a high performance lens (Gradium GPX085) to a spot size of approximately 55 μm for the 659-nm laser and 326 μm for the 830-nm laser. The modulated infrared PTR signal from the tooth was collected and focused by two off-axis paraboloidal mirrors onto a Mercury Cadmium Telluride (HgCdTe or MCT) detector (EG&G Judson J15D12-M204-S050U). Before being sent to the lock-in amplifier, the PTR signal was amplified by a preamplifier (EG&G Judson PA-300). For the simultaneous measurement of PTR and LUM signals, a germanium window was placed between the paraboloidal mirrors so that wavelengths up to 1.85 μm (Ge bandgap) would be reflected and absorbed, while infrared radiation with longer wavelengths would be transmitted. The reflected luminescence was focused onto a photodetector of spectral bandwidth 300 nm ~ 1.1 μm (Newport 818-BB-20). A cut-on colored glass filter (Oriel 51345, cut-on wavelength: 715 nm) was placed in front of the photodetector to block laser light reflected or scattered by the tooth. For monitoring the modulated luminescence, another lock-in amplifier (EG&G model 5210) was used. Both lock-in amplifiers were connected to, and controlled by, the computer via RS-232 ports.

In the case of the statistical approach, at each measurement point, a frequency scan was performed measuring the PTR and the LUM signals by varying the frequency from 1 Hz to 1 kHz while the depth profilometric experiments were performed by moving a sample along any axis at a fixed frequency. At any case, all signals were maximized by rotating the surface of the tooth exposed to laser light so that the incidence was nearly normal to the surface.

2.5 Histology Observation

After all the measurements were finished, the teeth in our sample were sectioned and photographed with the CCD camera directed perpendicular to the surface at each measurement point. The photographs of the sectioned teeth were examined and ranked according to the criteria listed in Table 1.

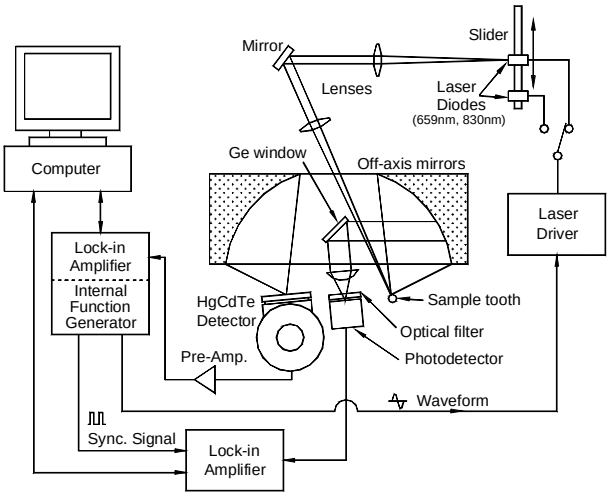

Fig. 1 Schematic diagram of experimental set-up for combined PTR and LUM monitoring.

3. RESULTS AND DISCUSSION

3.1 Statistical approach

In Fig. 2, this mandibular second premolar illustrates the typical diagnostic ability of PTR and LUM. The tooth had a DIAGNOdent reading of maximum 10 and average visual inspection ranking of 2.2 indicating that a clinician would need to watch or monitor the fissures. There was no indication on the radiographs of any caries being present. Nevertheless, PTR and LUM signals, including all information from the amplitude and phase responses over the entire frequency scan (1 Hz ~ 1 kHz), indicate that F2 and F3 have caries into dentin. Histological observation results show that this is, indeed, the case for these two points, as well as for point F1. The signals from fissure F1 show the influence that fissure geometry, angle of the mouth of the fissure, or the direction of the fissure base may have in the generation of PTR and LUM signals. The PTR amplitude of F1 in Fig. 2(f) is above the healthy band and the PTR phase in Fig. 2(g) also shows clear departure from the healthy band in the high frequency range. This case illustrates the depth profilometric abilities of PTR. Fig. 2(b) shows that the slanted carious fissure F1 was illuminated by the incident laser beam in such a way that the carious region formed a thin surface layer, succeeded by a much thicker healthy substrate enamel layer. In response, the phase of the PTR signal for F1, Fig. 2(g), falls within the healthy band at low frequencies as expected from the long thermal diffusion length which mostly probes the healthy enamel sub-layer with the carious surface layer as a perturbation to the signal. At high frequencies, however, the (short) thermal diffusion length lies mostly within the carious surface layer and, as a result, the PTR phase emerges below the healthy band above ca. 50 Hz and joins the phases of the carious spots F2 and F3. In principle, the frequency of departure from the healthy band can be used to estimate the thickness of the carious surface layer. PTR and LUM curves of the healthy fissure F4 are located within the healthy band confirming the histological observations.

In order to assess PTR and LUM as caries diagnostic techniques and compare them (combined and separately) to other conventional probes, sensitivities and specificities were calculated at two different thresholds (D_2) and (D_3) as defined in Table 1 for all the diagnostic methods. While the PTR and LUM signals were taken from all 280 occlusal measurement points, only 1 or 2 points on each tooth were assessed by the other examination methods. Therefore, each calculation only used the corresponding measurement points. To create suitable criteria for assessing the carious state via PTR and LUM, the general characteristics of the respective signals and their converting equations, listed in Table 2 were used. Those characteristics were established from the experimental results of the frequency scans with carious and healthy tooth samples. In the case of the PTR amplitude, the shape of the frequency scan curve for the healthy spot on a log-log plot is almost linear from low frequency (1 Hz) to high frequency (1000 Hz), while unhealthy spots (demineralized surface, enamel caries or dentin caries) exhibit larger amplitude than healthy spots over the entire frequency range and a pronounced curvature with a “knee” at certain frequency ranges on the logarithmic plot. The PTR phase shape for the healthy spot on a linear (phase) - log (frequency) plot is almost linear across all frequencies (1 Hz ~ 1 kHz), while unhealthy spots exhibit larger phases at low frequencies and large slopes, crossing the healthy phase range at intermediate frequencies. There is no difference in the LUM amplitude shape between healthy and unhealthy spots. The shape of the amplitude curves is consistent throughout, decreasing from low to high frequencies. The

LUM amplitude curves for unhealthy spots lie above the healthy band over the entire frequency range. The LUM phase shows slight differences between healthy points and carious points. In general, carious regions exhibit LUM phase lags slightly shifted above the healthy mean throughout the measured frequency range. Healthy spots may exhibit slight deviations, but only at the high frequency end (> 100 Hz).

We established the mean values for PTR amplitude and phase, and LUM amplitude and phase from all the healthy smooth surface points on the tooth samples. This allowed us to examine the behavior of healthy tooth structure without the influence of fissure geometry or the effects of varying enamel thickness in the fissure. A series of mean values and standard deviations vs. frequency curves were developed for each signal and plotted for each tooth. This allowed us to compare the behavior of each probed point to a healthy smooth surface area.

Using these features, characteristic (converting) equations were generated from the plots to yield numeric values defining the state of the teeth as listed in Table 2. In addition, out of the entire frequency scan, each signal (PTR and LUM amplitude and phase) was examined at 3 or 4 frequencies whether it deviated from the healthy norm band, and the number of points that deviated from this band was counted. After calculating all these values, each number group was normalized so that the assigned numbers in each group had a value between 0 for intact teeth and 1 for the worst case of caries. Then these normalized numbers were added and used to evaluate the probed spots. Finally, one value per each measurement point was recorded which included all available information of the frequency response. The thresholds of D_2 and D_3 were determined by trial and error to comply with the histological observations as closely as possible.

The results of the statistical analysis are given in Table 3. Using the combined criteria of PTR and LUM, the highest sensitivities and specificities, 0.81 and 0.87, respectively, were calculated at the D_2 threshold among all the examination methods. In the cases of PTR-only or LUM-only criteria, sensitivities are between 0.52 and 0.69, while specificities are relatively higher, between 0.72 and 0.86. In a manner similar to other researchers' findings[5,14-16], visual inspection resulted in poor sensitivities (0.51 at D_2 and 0.36 at D_3) and particularly high specificities (1.00 at both thresholds). Radiographs also exhibited poor sensitivities (0.29 at D_2 and 0.36 at D_3) and high specificities (1.00 at D_2 and 0.85 at D_3). The continuous (dc) luminescence method (DIAGNOdent) showed sensitivities of 0.60 at D_2 and 0.76 at D_3 ; specificities were 0.78 at D_2 and 0.85 at D_3. From Table 3 it should be noted, however, that a relatively small subset of all our measurement spots was used for obtaining the visual and radiographic statistics, compared to the much more comprehensive sample sizes used for the other methods, especially for PTR and LUM. In addition, DIAGNOdent measurements were performed with that instrument's fiber-optic waveguide, whereas LUM and PTR measurements used direct incidence of the light on the tooth surface and were subject to variable incidence solid angle limitations.

3.2 Depth profilometric experiments

3.2.1 Detection of artificial sub-surface hole at variable depths from tooth surface

A hole was drilled in the middle third of the tooth just at the base of two very deep fissures. Fig. 3(a) shows a cross-sectional view of the drilled hole in the sample at the end of the experiments and the depth of each hole from the scanned surface at each measured interval. The two holes to the right of the grooves are the bottoms of the fissures which were visible on the top surface. A magnified view of the scan line is shown in Fig. 3(b). The cross-section in Fig. 3(a) illustrates the changing mineral content as the dentin approaches the pulp chamber. Close to the pulp chamber, there is less mineralized tissue and more tubules containing tissue fluids and odontoblast processes. As shown in Fig. 3(c,d), the PTR amplitude and phase changed greatly when the first hole was made. The distance from the scanned surface (along the arrow on top of the picture in Fig. 3(b)) to the bottom of the drilled hole after the first drilling was approximately 5 mm. The large PTR signal scan change from the intact level is indicative of the depth-integral contributions to the PTR signal along the entire thickness (or substantial portion thereof) of the tooth. It seems to be caused by drilling out a large dark area (dentin very close to the pulp chamber) in the middle of the tooth with two distinct lobes corresponding to the two signal peaks. Vestiges of the area are still visible in Fig. 3(a). A major part of this deep slightly mineralized dentin was removed by the first drilling. As the hole was drilled farther, there were no comparably large changes in the PTR amplitude. It is hypothesized that this might be so because the major part of the dark region which was not as mineralized as the surrounding dentin had already been removed by the initial drilling. The LUM amplitude and phase in Fig. 3(e,f) also show substantial differences after the first drilling, albeit with much less contrast and not as extensive as the PTR signals. Since the tooth is a turbid medium, optical penetration is controlled by scattering and the PTR signal depth sensitivity is not limited to the theoretical thermal diffusion length

$\mu = \sqrt{\alpha/(\pi f)}$, where α is the material thermal diffusivity (cm^2/s) and f is the laser modulation frequency (Hz). μ is approximately 386 μm at 1 Hz and 12 μm at 1 kHz; the thermal diffusivity of enamel is 4.69×10^{-3} cm^2/s [17]. The thin enamel surface was broken away when the drill tip reached the surface (thickness = 0 mm), and the PTR amplitude around the gaping hole increased due to the very thin enamel layer and edge effects[18]. With these results, it was concluded that PTR and LUM are able to detect sub-surface defects or changes in mineralization with sharp boundaries at depths greater than 5 mm, with PTR exhibiting superior sensitivity and contrast to both the presence of, and changes in, the sharp boundaries, as well as changes in mineral content (dark regions) of the tooth.

Table 2. Characteristics of frequency scan curves of PTR and LUM

Signal	General characteristics	Converting equation to determine numeric ranking
PTR amplitude	The shape for a healthy spot in log-log plot is almost linear from low frequency (1 Hz) to high frequency (1000 Hz). Unhealthy (demineralized surface, enamel caries or dentin caries) spots show greater amplitude at all frequency ranges compared to healthy spots. Unhealthy spots show a curvature (greater than healthy spots) in the frequency range of 10 ~ 100 Hz in a logarithmic plot.	(slope at low frequency) – (slope at high frequency) average of 4 frequencies
PTR phase	The shape for the healthy spot in log (freq.) - linear (phase) plot is almost linear from low frequencies (1 Hz) to high frequencies (1000 Hz). Unhealthy spots show higher phase at low frequency range and the reverse at the high frequency range than healthy spots.	(average of phases at 2 low frequencies (1, 6.68 Hz)) – (average of phases at 2 high frequencies (211.35, 1000 Hz))
LUM amplitude	Both healthy and unhealthy spots show same shape: higher amplitude at low f than at high f. Unhealthy spots show greater amplitude than healthy ones.	average at 3 frequencies (1, 211.35, 501.18 Hz)
LUM phase	High frequency range (> 100 Hz) only, unhealthy spots show larger phase than healthy ones.	one phase signal at high frequency (501.18 Hz)

Table 3. Sensitivities and specificities at the caries level of enamel (D_2) and the caries level of dentin (D_3) for various examination methods

Examination method	Sensitivity threshold (D_2/D_3)	Specificity threshold (D_2/D_3)	Size of sample (# of points)
PTR and LUM combined	0.81 / 0.79	0.87 / 0.72	280
PTR only	0.69 / 0.52	0.86 / 0.72	280
LUM only	0.61 / 0.58	0.81 / 0.77	280
Visual Inspection	0.51 / 0.36	1.00 / 1.00	52
Radiograph	0.29 / 0.36	1.00 / 0.85	52
DIAGNOdent	0.60 / 0.76	0.78 / 0.85	131

3.2.2 Deep sub-surface carious lesion in dentin

The horizontal cross-section of a mandibular central incisor with a large carious lesion on both interproximal surfaces is shown in Fig. 4(a). Fig. 4(b) is a view of the horizontal cross-section at a level indicated by the arrow in Fig. 4(a). It shows (high-lighted) the carious lesion involving most of the dentin, and a section of the pulp horn just beneath the dentin surface. The white area within the high-lighted region is actually dentin that is not highly mineralized since it is very near the pulp and contains a large number of tubules, much higher than dentin near the DEJ. The arrow in Fig. 4(b) shows the direction and extent of the laser scan across the intact side surface of the tooth corresponding to the arrow in Fig. 4(a). The spatial scan results with the 659-nm laser as a source modulated at 5 Hz are shown in Fig. 4(c). From the onset to the middle of the scan, the PTR amplitude is high (5×10^{-4} V range) over the region which is consistent with the presence of the deep sub-surface lesion at approx. 2.5 mm below the tooth surface. The PTR signal drops to ca. 5×10^{-5} V outside the carious region and rises slightly again close to the right edge of the tooth (a thermal-wave edge effect[27]). The LUM amplitude also shows similar structure but far less dramatic contrast than the PTR amplitude, a further indication of the non-depth-profilometric nature of modulated luminescence as signal strength is weighed equally from all sub-surface depths. The difference in sensitivity to the deep sub-surface lesion between PTR and LUM is that the PTR is more sensitive to deeper inhomogeneities than LUM even when sharp boundaries are involved. The low-frequency (< 100 Hz) insensitivity of the LUM phase, Fig. 4(d), to sub-surface dental structure has been noted earlier[19].

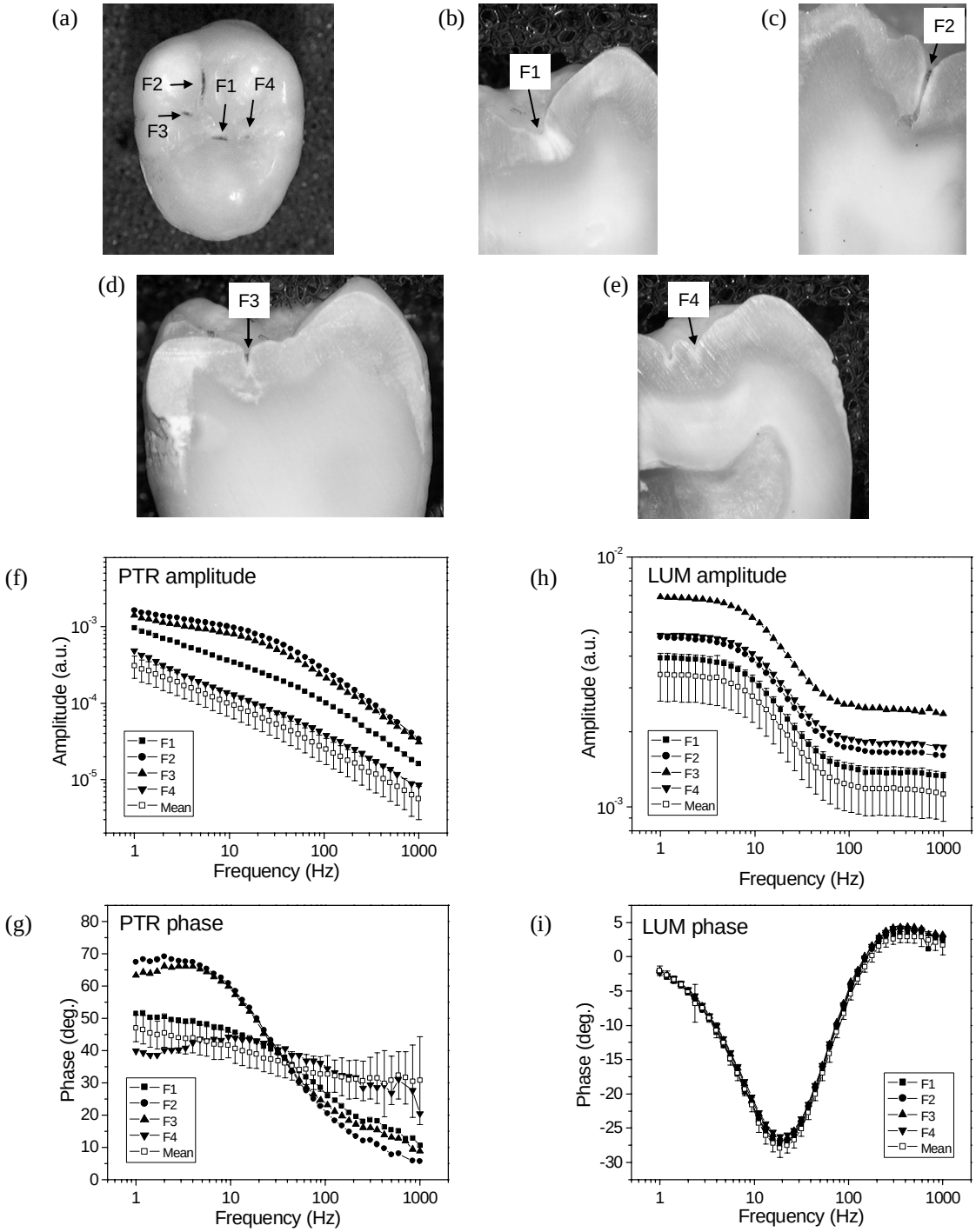

Fig. 2 A carious tooth sample and its PTR and LUM signals using 659-nm excitation. (a) occlusal view of the tooth; (b-e) cross sectioned view of each measurement point, F1, F2, F3 and F4; (f,g) PTR and (h,i) LUM amplitude and phase frequency scans at all the measurement points with the healthy mean value and population-weighted standard deviation.

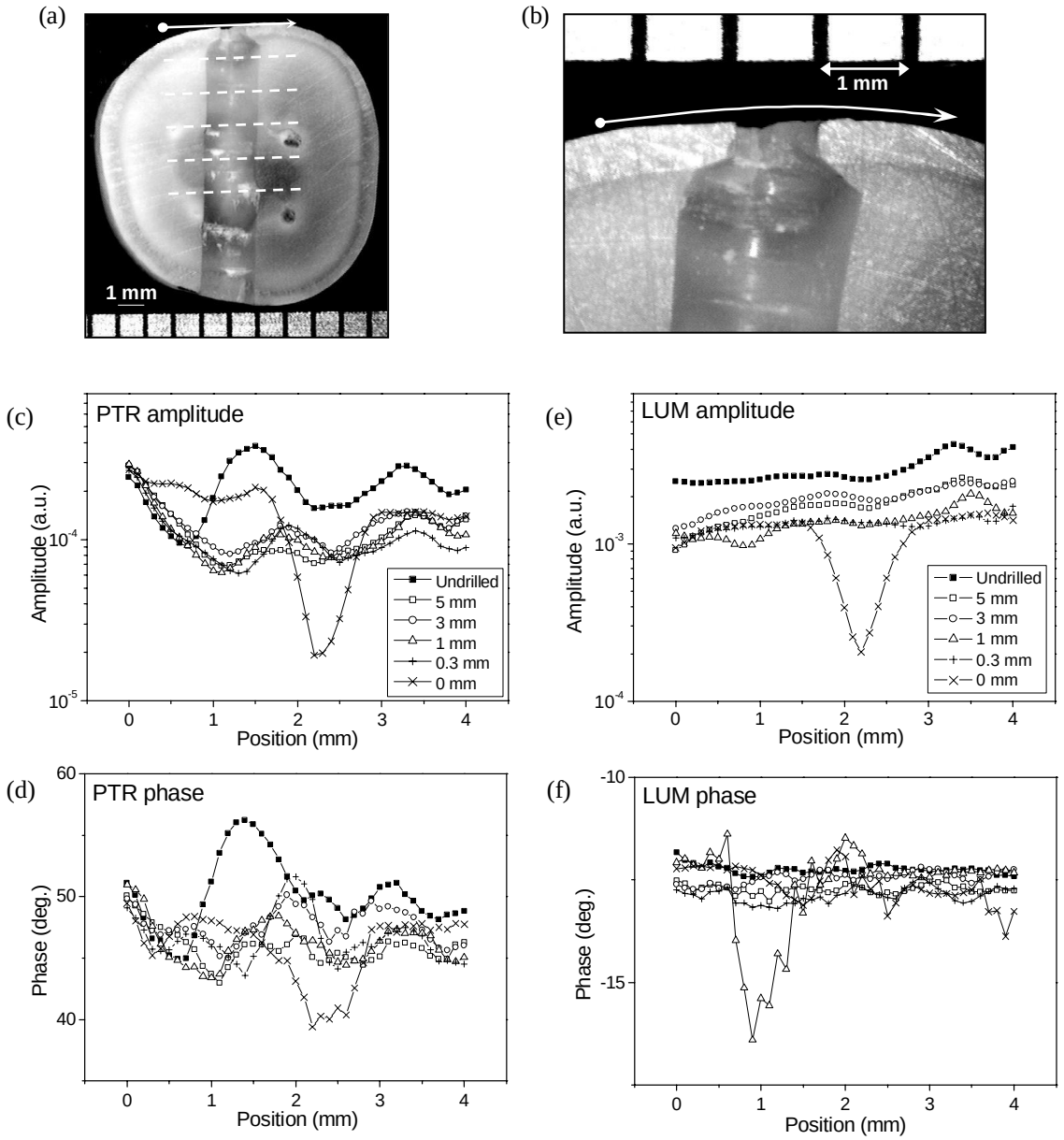

Fig. 3 Cross-sectional photographs and experimental results of a sample tooth for drilled hole detection. (a) transverse cross-section at the scan line along the center of a drilled hole; Magnified view of the whole cross section (white arrow is the scanning line and white dotted lines show the depths from the scanned surface, 1mm for each) (b) magnified view of laser scan across the drilled hole region (white arrow); (c,d) PTR amplitude and phase signals across the scan line at various depths of the tip of the drilled hole. The inset indicates distances from the scanned surface; (e,f) LUM amplitude and phase signals.

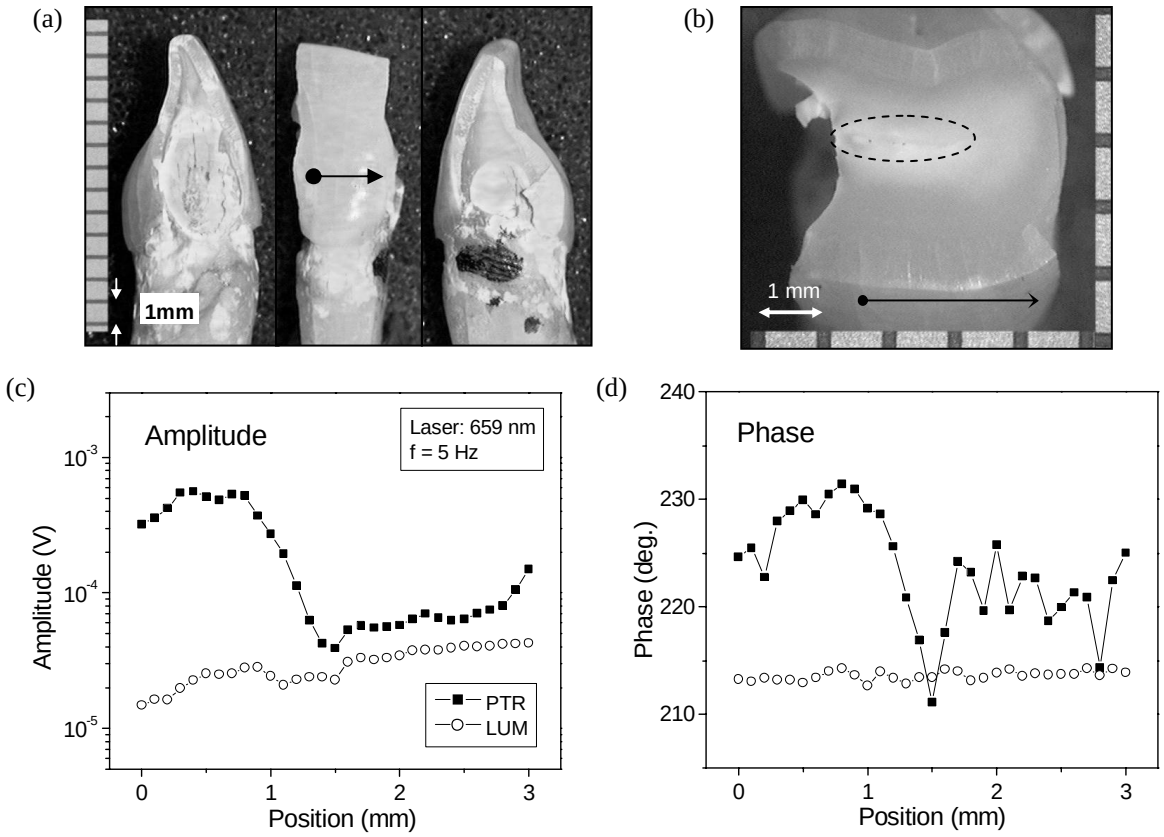

Fig. 4 Photographs and experimental results of the sample tooth having deep sub-surface carious lesion in dentin. (a) left, front, and right views of a mandibular incisor. (b) cross-section at the scan line at the level of the arrow in (a), highlighting a deep demineralized lesion (dotted region in the middle); (c,d) PTR and LUM amplitude and phase signals across the scan line at 5 Hz and 659 nm.

3.2.3 Enamel cracks

The tooth shown in Fig. 5(a) is healthy but there is a natural radial crack in the thick enamel as shown on the top-down cross-sectional plane of Fig. 5(b). The spatial scan results along the white arrow with the 659-nm laser at 5 Hz are shown in Fig. 5(c). Dashes in Fig. 5(b) have been added at the enamel-dentin junction to aid the eye. A sharp PTR amplitude peak and a shallow, broadened, LUM amplitude peak caused by the crack are shown around 2.8 mm from the scan onset coordinate point. PTR shows higher spatial resolution and contrast than LUM because the latter is more sensitive to scattered excitation light at the crack which broadens the region from which multi-scattered luminescence photons are collected. The PTR signal is primarily due to the thermal discontinuity in the cracked region which occurs along the actual crack configuration and is thus more representative of the actual crack extent. The fact that there are no significant changes in the PTR phase scan, indicates that thermal-wave flux disruption occurs mainly sideways as the laser beam sweeps across the walls of the crack, rather than impeded flux along the depth coordinate, a phenomenon well-known from Mirage-effect measurements in the non-destructive evaluation of cracks in engineering materials[10,11]. Unfortunately, the expected small phase variation from the lateral thermal impedance represented by the crack wall is lost in the noise of Fig. 5(d), as the overall healthy tooth generates low PTR signals less than 10^{-4} V. It has been found that, as a rule, healthy and thick enamel generates small PTR and LUM amplitudes (< 0.1 mV). The LUM phase shows no contrast, consistently with the insensitivity of this signal channel to dental irregularities at low frequencies. In summary, successful PTR detection of natural sub-surface cracks in teeth, also reported earlier[8], depends on the size, orientation and depth of the crack. LUM detection is unpredictable and may possibly distort the geometric shape of the crack.

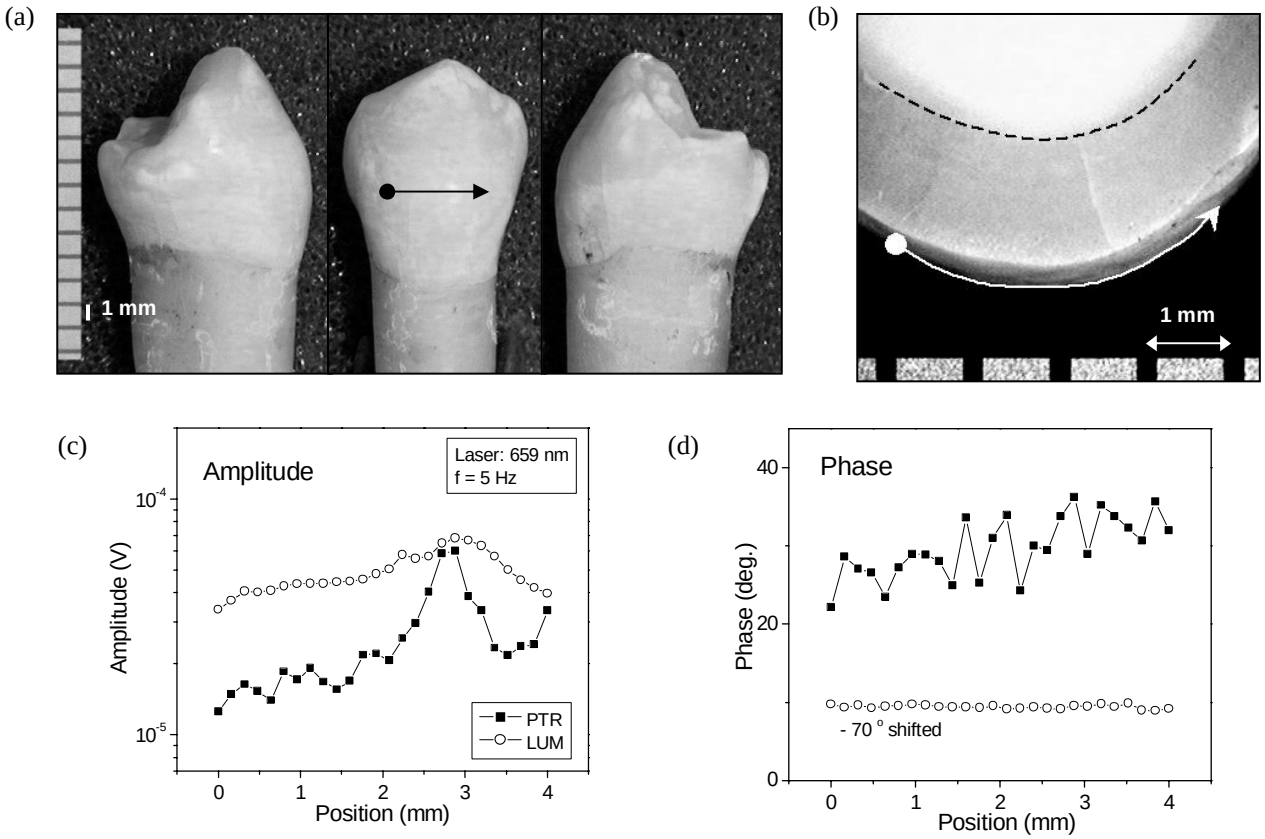

Fig. 5 Photographs and experimental results of a mandibular bicuspid with a radial enamel crack. (a) left, front, and right views of the tooth; (b) cross section at the scan level showing the radial crack. The DEJ is highlighted to aid the eye; (c,d) PTR and LUM amplitude and phase signals across the scan line at 5 Hz.

4. CONCLUSIONS

In conclusion, the combined wealth of information stemming from four PTR and LUM signals (two amplitudes and two phases), including the availability of detailed frequency response curve shapes over a wide range of modulation frequencies, was used to examine a large number of spots (280) representing fifty two teeth. The combined PTR/LUM approach yielded a statistical sensitivity higher than any of the other methods used in this study, and a specificity comparable to that of dc luminescence diagnostics, although comparisons with DIAGNOdent, radiography and visual inspection results was made using for the latter methods only a subset of the full set of dental spots examined with PTR/LUM.

PTR depth profilometric capability within depths at least 5 mm below the enamel surface was demonstrated by means of artificial sub-surface hole drilling. Some natural defects such as a deep sub-surface carious lesion in dentin and a crack have been shown to be detected by this technology. Also more penetrating laser radiation at 830 nm exhibits better PTR resolution and contrast of scanned sub-surface carious features than 659-nm radiation at some expense of signal magnitude and signal-to-noise ratio at high frequencies. The imaging potential of the same features using LUM was shown to be less promising.

It is concluded that combined PTR and LUM have excellent potential to become a sensitive, non-intrusive, depth-profilometric dental probe for the diagnosis of near-surface or deep sub-surface carious lesions.

ACKNOWLEDGMENTS

The support of Materials and Manufacturing Ontario (MMO) is gratefully acknowledged.

REFERENCES

1. McComb D and Tam LE: Diagnosis of Occlusal Caries: Part I. Conventional Methods. J Can Dent Assoc 2001;67:454-457
2. Eggertsson H, Analoui M, van der Veen MH, González-Cabezas C, Eckert GJ, and Stookey GK: Detection of Early Interproximal Caries in vitro Using Laser Fluorescence, Dye-Enhanced Laser Fluorescence and Direct Visual Examination. Caries Res 1999;33:227-233.
3. Lagerweij MD, van der Veen MH, Ando M, Lukantsova L, and Stookey GK: The Validity and Repeatability of Three Light-Induced Fluorescence Systems: An In vitro Study. Caries Res 1999;33:220-226.
4. Hibst R, Konig K: Device for Detecting Dental Caries. US Pat 1994; 5,306,144.
5. Alwas-Danowska HM, Plasschaert AJM, Suliborski S and Verdonschot EH: Reliability and validity issues of laser fluorescence measurements in occlusal caries diagnosis. J Dentistry 2002;30:129 – 134.
6. Lussi A, Imwinkelried S, Pitts NB, Longbottom C, and Reich E: Performance and Reproducibility of a Laser Fluorescence System for Detection of Occlusal Caries in vitro. Caries Res 1999;33:261-266.
7. Mandelis A, Nicolaides L, Feng C, and Abrams SH: Novel Dental Depth Profilometric Imaging Using Simultaneous Frequency-Domain Infrared Photothermal Radiometry and Laser Luminescence; in Oraevsky A (ed): Biomedical Optoacoustics. Proc SPIE, 2000, vol 3916, pp 130-137.
8. Nicolaides L, Mandelis A, and Abrams SH: Novel Dental Dynamic Depth Profilometric Imaging Using Simultaneous Frequency-Domain Infrared Photothermal Radiometry and Laser Luminescence. J Biomed Opt 2000;5:31-39
9. Mandelis A: Review of progress in theoretical, experimental, and computational investigations in turbid tissue phantoms and human teeth using laser infrared photothermal radiometry; in Maldague XP and Rozlosnik AE (ed): Thermosense XXIV, Proc SPIE, 2002, vol 4710, pp 373-383.
10. Busse G and Walther HG: Photothermal nondestructive evaluation of materials with thermal waves; in Mandelis A (ed): Principles & Perspectives of Photothermal & Photoacoustic Phenomena. Elsevier, New York, 1992, vol 1, pp 205-298.
11. Munidasa M and Mandelis A: Photothermal Imaging and Microscopy; in Mandelis A (ed): Principles & Perspectives of Photothermal & Photoacoustic Phenomena. Elsevier, New York, 1992, vol 1, pp 299-367.
12. Nicolaides L, Feng C, Mandelis A, and Abrams SH: Quantitative dental measurements by use of simultaneous frequency-domain laser infrared photothermal radiometry and luminescence. Appl Opt 2002;41:768-777.
13. Jeon RJ, Mandelis A, Sanchez V, and Abrams SH: Non-intrusive, Non-contacting Frequency-Domain Photothermal Radiometry and Luminescence Depth Profilometry of Carious and Artificial Sub-surface Lesions in Human Teeth. J Biomed Opt 2003 (accepted).
14. Heinrich-Weltzien R, Weerheijm KL, Kühnisch J, Oehme T and Stösser L: Clinical evaluation of visual, radiographic, and laser fluorescence methods for detection of occlusal caries. J Dent Child 2002;69:127-132.
15. Costa AM, Yamaguchi PM, De Paula LM and Bezerra ACM: In vitro study of laser diode 655 nm diagnosis of occlusal caries. J Dent Child 2002;69:249-253.
16. Lussi A, Megert B, Longbottom C, Reigh E, Francescut P: Clinical performance of a laser fluorescence device for detection of occlusal caries lesions. Eur J Oral Sci 2001;109:14-19.
17. Brown WS, Dewey WA and Jacobs HR: Thermal Properties of Teeth. J Dent Res 1970;49:752-754.
18. Mandelis A: Diffusion-Wave Fields: Mathematical Methods and Green Functions. Springer, New York, 284-296, 2001.